Journal of Hydrology 620 (2023) 129452

Contents lists available at ScienceDirect

Journal of Hydrology

journal homepage: www.elsevier.com/locate/jhydrol

Research papers

Impacts of drought and heat events on vegetative growth in a typical humid zone of the middle and lower reaches of the Yangtze River, China

Huiming Han [a,b], Hongfu Jian [a,b], Mingchao Liu [a,c], Sheng Lei [d], Siyang Yao [c,*], Feng Yan [c,*]

[a] Jiangxi Academy of Water Science and Engineering, Nanchang 330029, China
[b] Jiangxi Provincial Technology Innovation Center for Ecological Water Engineering in Poyang Lake Basin, Nanchang 330029, China
[c] Key Laboratory of Poyang Lake Environment and Resource Utilization, Nanchang University, Ministry of Education, Nanchang 330031, China
[d] Jiangxi Water Conservancy Bureau, Nanchang 330029, China

ARTICLE INFO

Keywords:
Extreme meteorological event
Vegetation growth
Interactive effect
Geographic detector

ABSTRACT

Due to climate change, the frequencies of extreme meteorological events have increased around the world over the last few decades, which would significantly affect the growth of vegetation, especially in humid regions. However, few previous studies have investigated the effects of compound extreme meteorological events on the growth of vegetation, such as compound drought and heat events (CDHEs). In this research, we assessed the individual and interactive impacts of drought and heat events on the growth of vegetation using geographic detectors in the Poyang Lake Basin (PYLB), which is located in a typical humid zone in the middle and lower reaches of the Yangtze River (MLYR) of China. We found that the effect of heat events on the growth of vegetation was greater than that of drought events in this region. Among the various vegetation types, shrubland (SL) and cultivated vegetation (CV) were most significantly affected by drought and heat events, respectively, and broadleaf forest (BLF) was more tolerant of drought (heat) events than other vegetation. Drought events had significantly negative effects on the growth of vegetation, and needle-leaf (NLF) and BLF exhibited a two-month lagged response. The impact of CDHE on the growth of vegetation was remarkably stronger than that of a single event, and the interaction type was bi-factor enhanced or nonlinear enhanced. Our findings highlight the need to consider CDHEs when assessing the response of vegetation to climate extremes under global warming.

1. Introduction

The hydrological cycle is intensifying as the climate warms, thereby leading to more frequent extreme climate events (Fischer et al., 2021; Nangombe et al., 2018). Extreme weather events are forecast to grow more frequent and more spatially widespread in the future (Diffenbaugh et al., 2015; Skinner et al., 2018). Vegetation is a sensitive indicator of climate change and it may be severely threatened. Meanwhile, vegetation is a vital dynamic part of the terrestrial and atmospheric systems, and it may affect the underlying surface conditions, water vapor cycle, and carbon cycle (Christopher et al., 2018; Sungmin et al., 2022). The growth of vegetation is influenced and constrained by climatic conditions, and a suitable combination of water and heat is important for its growth (Nemani et al., 2003). The vegetation is abundant and varied in the humid zones, and this area has a high incidence of droughts, heat waves, and other events (Ning et al., 2022; Wu and Jiang, 2022; Chen et al., 2021; Liu et al., 2022a). For example, the middle and lower reaches of the Yangtze River (MLYR) experienced an unprecedented drought and heat event during the summer and fall in 2022. These events can affect various vegetation growth processes, including photosynthesis, breathing action, and carbon utilization, thereby result in leaf senescence and mortality (Reichstein et al., 2013; Teskey et al., 2015; Berdugo et al., 2020). Therefore, it is important to investigate the effects of extreme meteorological events on vegetation in humid areas.

Precipitation and temperature are the key climatic factors that affect the growth of vegetation, and climate anomalies (or drought and heat) are mostly represented using indices of drought (e.g., standardized precipitation index (SPI)) and heat (standardized temperature index (STI)) (McKee et al., 1993; Vicente-Serrano et al., 2010; Zscheischler et al., 2017a). These indices have been applied widely to assess drought or heat events at global or regional scales. Over recent decades, many studies have been conducted to improve our understanding of the impacts of drought or heat on vegetation (Miller et al., 2022; Li et al., 2021; Baumbach et al., 2017; Gampe et al., 2021; Zhang et al., 2022). For

* Corresponding authors.
E-mail addresses: jxnc202222@163.com (H. Han), ysy2003003@163.com (S. Yao), yfmilan@163.com (F. Yan).

https://doi.org/10.1016/j.jhydrol.2023.129452

Available online 28 March 2023

example, Wang et al. (2022) investigated the effects of drought events on the normalized difference vegetation index (NDVI) for vegetation in Inner Mongolia and found that the probability of NDVI degradation increased with the degree of drought. Xu et al. (2019) showed that the impacts of extreme droughts on vegetation productivity will increase further under climate change. Rita et al. (2020) investigated the impacts of the European summer drought in 2017 on the vegetation NDVI and found marked differences in the responses of different types of vegetation to drought, where these differences were closely linked to elevation. Dong et al. (2022) found that heat events slowed the growth in the vegetation NDVI on the Tibetan Plateau, and the growth of vegetation was more sensitive to heat events in June than July and August. Zhang et al. (2015) indicated that different types of vegetation vary in terms of their sensitivity to extreme heat. Drought and heat events may occur simultaneously and the two may interact, but previous studies mainly assessed the separate effects of drought or heat events on vegetation. Droughts and heat rarely occur separately, and thus, they should be regarded as compound extreme events (Zscheischler et al., 2017b) that may have greater impacts than individual extreme events (Wu et al., 2021). Therefore, some studies have investigated the impacts of CDHEs. Kang et al. (2022) found that the desert steppe region was most affected by CDHEs in Inner Mongolia. Li et al. (2021) showed that the impact of CDHEs on vegetation loss increased as the air temperature increased from June to August in Xinjiang. However, CDHEs are becoming more frequent and severe, and their effects on vegetation growth require further investigation.

Most previous studies that examined the effects of droughts (heats) on the vegetation NDVI employed correlation analysis, regression analysis methods, and trend analysis (Ge et al., 2021; Xiong et al., 2021; Zhang et al., 2016; Zhang et al., 2017; Zhan et al., 2022; Rousta et al., 2020). However, these studies assumed significant linear relationships between certain factors and vegetation over a time series, but the response of growth by terrestrial vegetation to various factors can be complex and linear statistical methods may not accurately describe the relationships between vegetation and certain variables (Peng et al., 2019; Zhou et al., 2022; Zhao et al., 2019). Copula–based models have recently been applied to investigate the interactive effects of droughts and heats on vegetation (Li et al., 2021), but this approach is unable to discern how drought and heat events interact, or explain the spatial heterogeneity of plant responses to extreme events. The geographic detector pattern is considered a potential approach for researching the spatial heterogeneity of growth by vegetation and related factors, where it can identify the significance and extent of various types of drivers (meteorology, geography, human activities, etc.) and explain their interactive effect on vegetation. However, this model has not been widely tested for analyzing the effects of droughts and heats on the capacity for growth by vegetation.

The Poyang Lake Basin (PYLB) is located in the MLYR in southern China, and this area has high vegetation cover due to the implementation of forest restoration and ecological restoration projects. The types of vegetation in the PYLB are diverse, but broadleaf forest (BLF), needleleaf forest (NLF), and scrubland (SL) predominate. Numerous national nature reserves are present in the PYLB, including Wuyi Mountain, Jiuling Mountain, and Luoxiao Mountain. Ecological resources are abundant and the terrestrial vegetation ecosystem is an important green ecological barrier in the MLYR. The region is in a humid subtropical zone with abundant but highly uneven seasonal precipitation, and thus drought and heat events are frequent and they can have severe impacts on the growth of vegetation.

Therefore, we studied the impacts of droughts and heats on the growth of vegetation in the PYLB, as a typical humid region in southern China, to improve our understanding of the potential reactions of vegetation to climate change. The main aims of our research were: (1) to determine the relative effects of drought events and heat events on growth by different types of vegetation; and (2) to quantitatively estimate the interactive effects of drought and heat events on the growth of different vegetation types.

2. Datasets and methods

2.1. Study area

The PYLB is on the south side of MLYR between 113°42′–118°30′E and 24°29′–30°05′N (Fig. 1). This area has a subtropical humid climate, which is influenced by the East Asian monsoon and South Asian monsoon. The PYLB is one of the eight major subsections of the Yangtze River Basin, with a basin area of 162,225 km^2 and it accounts for 9 % of the total basin. The PYLB comprises Poyang Lake, the largest fresh lake in China, and five rives system flood into the lake. The terrain is low in the middle but high in the surrounding area, thereby forming a relatively complete large watershed ecosystem.

2.2. Datasets

In this study, NDVI data and vegetation type data for the PYLB were obtained from the Resource and Environmental Sciences and Data Center, Chinese Academy of Sciences (http://www.resdc.cn). The PYLB has suffered more severe drought and heat events over the last two decades than previously, so we focused on CDHEs that occurred in this region over the last two decades (Gampe et al., 2021; Liu et al., 2022a). NDVI was used to characterize the vegetation growth state. Based on SPOT/VEGETATION NDVI satellite remote sensing data from 1998 to 2019, the maximum combination approach was commonly used to reduce the effects of cloud cover and other interfering factors, and the NDVI was converted into monthly data with a resolution of 1 km. These data effectively reflect the changes in vegetation cover and growth, and they have been widely employed for vegetation monitoring, forestry utilization, and other purposes (Chen et al., 2022). In addition, we used the 1:1,000,000 Vegetation Atlas of China. We focused on the five most common planting cover types in PYLB comprising cultivated vegetation (CV), NLF, grassland (GL), BLF, and SL (Fig. 2). We used monthly meteorological data, including precipitation and temperature, from 34 national basic meteorological stations in the PYLB from 1998 to 2019. These data were obtained from Jiangxi Meteorological Information Center.

2.3. Methods

2.3.1. Identification of extreme climatic events

One-month time scale SPI and STI data were used to characterize drought and heat events during 1998–2019, where they captured the short-term responses of relevant vegetation to surface fluxes (Zscheischler et al., 2017a). SPI and STI were calculated following the same procedure. They were computed by fitting the marginal distribution of monthly cumulative rainfall (temperature) to get the probability, p, which was then converted to a standard variable according to a standardized normal distribution, ω (i.e.,$\mathrm{STI} = \omega^{-1}(p)$). The marginal probability, p, of SPI (STI) was evaluated using the empirical Weibull plotting position (Feng et al., 2021). To determine whether a basin-wide drought (heat) event occurred based on the average SPI (STI) for all stations in the PYLB. $\mathrm{SPI} \leq -0.5$ indicated a drought event and $\mathrm{STI} \geq 0.5$ indicated a heat event (Hao et al., 2020; Han et al., 2018). All drought and heat events during the study period could be identified using SPI and STI, but some of these drought and heat events were not temporally synchronized. We screened out drought and heat events that were temporally coherent ($\mathrm{SPI} \leq -0.5$ and $\mathrm{STI} \geq 0.5$) and defined their combination as CDHE.

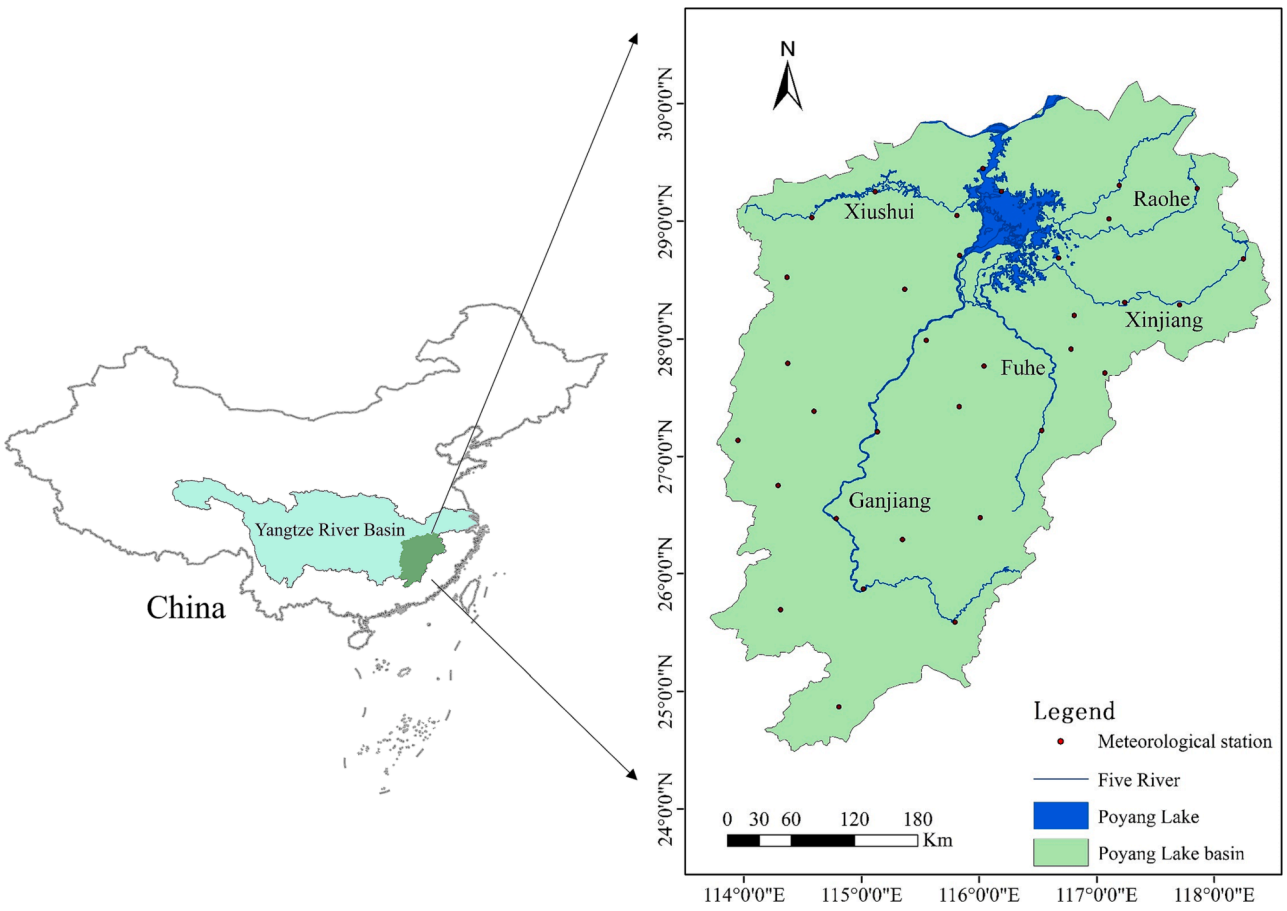

Fig. 1. Distribution of meteorological stations and geographical location of PYLB.

2.3.2. Identification of vegetation growth

We calculated the variation in NDVI (V_{NDVI}) under the condition of CDHEs on a monthly scale to represent the growth or decline of vegetation, as follows:

$$V_{NDVI_0} = NDVI_i - NDVI_{i-1} \quad (1)$$

where V_{NDVI_0} denotes the change in NDVI when vegetation did not exhibit a lagged response to drought (heat) event and i is the time (month) comprising the month when the CDHE occurred.

The change in the vegetation in the PYLB is considered to exhibit a lag time of 1–2 months in response to precipitation and temperature (Tan et al., 2015; Jiang et al., 2022). Thus, we calculated the response of the V_{NDVI} for vegetation with lags of one and two months under drought and heat conditions by using the following formulae:

$$V_{NDVI_1} = NDVI_{i+1} - NDVI_i \quad (2)$$

$$V_{NDVI_2} = NDVI_{i+2} - NDVI_i \quad (3)$$

where V_{NDVI_1} and V_{NDVI_2} are the changes in vegetation growth with lags of one month and two months under drought and heat conditions, respectively, and i is the time (month) comprising the month when the CDHE occurred.

In addition, we calculated the spatial correlation between each drought (heat) event and vegetation V_{NDVI} to reflect the direction of the effect of a drought (heat) event on the growth of vegetation. Spearman correlation and 95 % significance tests were used for further analyses. A positive spatial correlation between SPI and V_{NDVI}, i.e., V_{NDVI} decreased with the intensity of drought events, indicated that a drought event had an inhibitory effect on the growth of vegetation. A positive spatial correlation between STI and V_{NDVI}, i.e., V_{NDVI} increased with the intensity of the heat event, indicated that a heat event promoted the growth of vegetation, and vice versa.

2.3.3. Quantifying single and interactive effects of extreme climate events on vegetation

Both drought and heat affect the growth of vegetation, and they may also interact to affect vegetation. Therefore, the factor detector and interaction factor blocks in the geographic detector were used to analyze the single and interactive effects of drought and heat events on the growth of vegetation, respectively. The geographic detector requires discretization of the input, so it was necessary to discretize the drought (heat) events. Based on the ArcGIS platform, SPI and STI were divided into nine categories by using the natural break point method, and 12,344 effective sampling points were generated in the study area. The spatial correlation data for 12,344 sampling points were obtained by overlaying V_{NDVI}, SPI, STI, and vegetation type data during the CDHE periods in the study area.

The geographic detector is a spatial statistical model that can effectively detect spatial heterogeneity and its related pattern (Wang et al., 2017). This model involves overlaying the geographical distribution of variables x (SPI and STI) and y (V_{NDVI}) in space to account for the geographical heterogeneity of V_{NDVI} caused by SPI and STI (Fig. 3). The explanatory power is calculated as follows:

$$q = 1 - \frac{\sum_{i=1}^{j} N_i \sigma_i^2}{N\sigma^2} \quad (4)$$

where j is the classification of SPI and STI, N_i and σ_i^2 express the cell counts and the variance of V_{NDVI} at i–layer respectively, N and σ^2 express the cell counts and the variance of V_{NDVI} in the whole PYLB, and q express the affected degree of drought and heat events for changes in

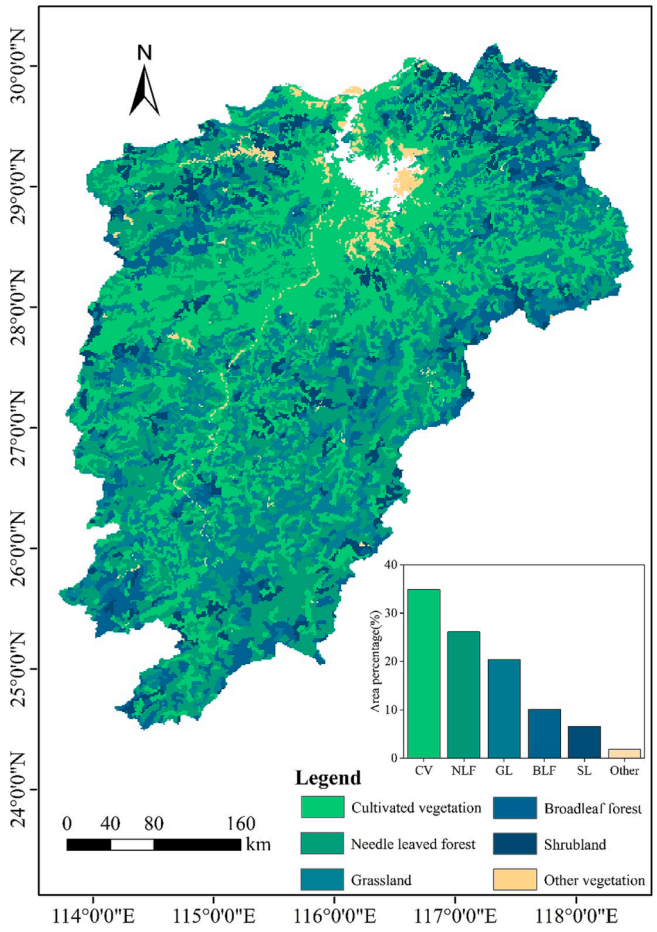

Fig. 2. Vegetation type distribution map. Note: CV, NLF, GL, BLF, and SL represent cultivated vegetation, needle-leaf forest, grassland, broadleaf forest, and shrubland respectively.

NDVI, $q \in [0, 1]$, where a larger value of q denotes stronger explanatory power, and vice versa.

Interaction detection is used to identify the interactions between factors, i.e., to identify whether the effects of drought events and heat events together (CDHEs) on vegetation will be stronger or weaker than that of separate drought events (heat events), or whether the effects of drought events and heat events on vegetation are independent of each other. The evaluation method involves comparing the single factor's q value (q(drought), q(heat)) and the combined effect (q(drought ∩ heat)). When q(drought ∩ heat) > q(drought) + q(heat), the interaction mode is enhanced in a nonlinear manner. When q(drought ∩ heat) = q(drought) + q(heat), the mode is independent. When q(drought ∩ heat) > Max(q(drought), q(heat)), the mode is bi–factor enhanced. When Min(q(drought), q(heat)) < q(drought ∩ heat) < Max(q(drought), q(heat)), the mode is single factor weakened. When q(drought ∩ heat) < Min(q(drought), q(heat)), the mode is weakened in a nonlinear manner.

3. Results

3.1. Spatial distribution of drought and heat events

First, we identified watershed-based drought and heat events during the vegetation growing season in 1998–2019, which occurred over 31 and 110 months, respectively, based on the one-month SPI and STI indices. In total, 15 CDHEs were identified based on the temporal consistency of the drought and heat events (Figs. 4 and 5). These CDHEs generally occurred between July and September, with an average occurrence frequency of about one and a half years. Heat events occurred frequently in the summer and autumn every year, and the precipitation had obvious seasonal characteristics. Drought events tended to occur frequently after the end of the rainy season in July, which was also the period when CDHEs often occurred. Among these CDHEs, the difference in the spatial distribution of drought events was more obvious than that of heat events. In addition, there were large differences in the intensity of droughts among different regions of the basin, whereas the differences were small for heat events. Severe drought events occurred in September 2001, July 2003, and September 2019, and severe heat events occurred mainly in July 2003, July 2007, and August 2019.

3.2. Effects of drought and heat events on vegetation

Differences in the physical structure of different vegetation types determine their susceptibility and tolerance to different drought heat events. Thus, we used factor detector analysis with geographic detectors to investigate the impacts of drought and heat events on the growth of the main types of vegetation (CV, NLF, GL, BLF, and SL) in the PYLB. To illustrate the effects of different drought and heat events on the growth of vegetation, Fig. 6 shows a bar chart depicting the effects of different drought and heat events on the five main types of vegetation individually during the growing season. The single factor explanatory power (q) of the effect of heat events on vegetation was 0.170, which was greater than that for the effect of drought events on vegetation (0.160), thereby indicating that the effect of heat events on the growth of vegetation was stronger than that of drought events in this region. For different types of vegetation, the single factor explanatory power (q) of the effect of drought events on SL was largest at 0.191. The mean value of the explanatory power (q) of the effect on BLF was 0.140. The mean

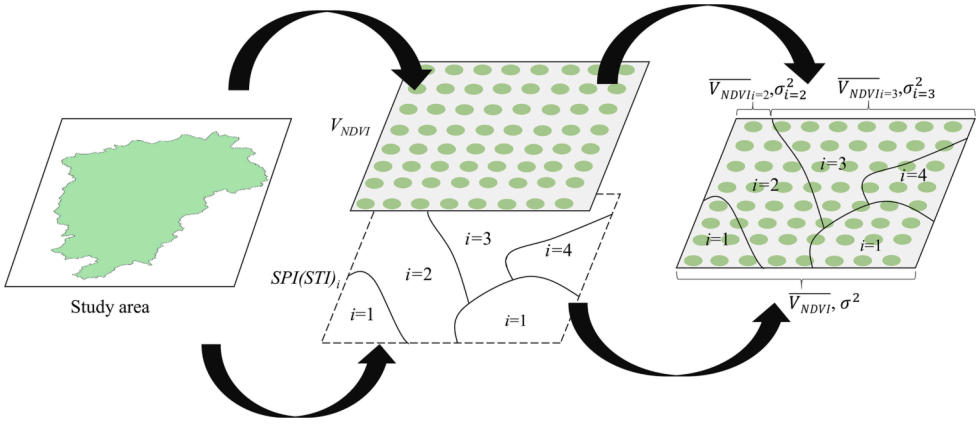

Fig. 3. Schematic illustration of the geographic detector.

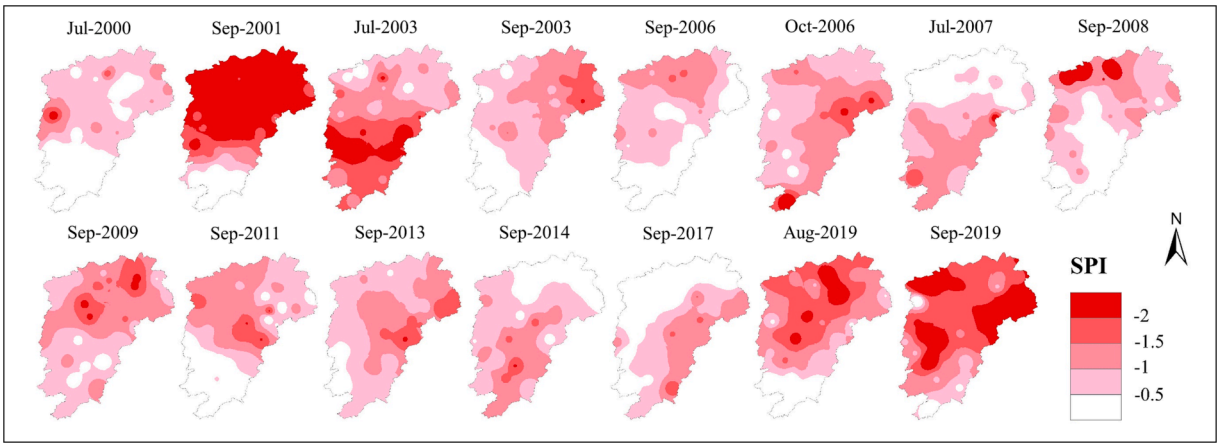

Fig. 4. Spatial patterns of drought events.

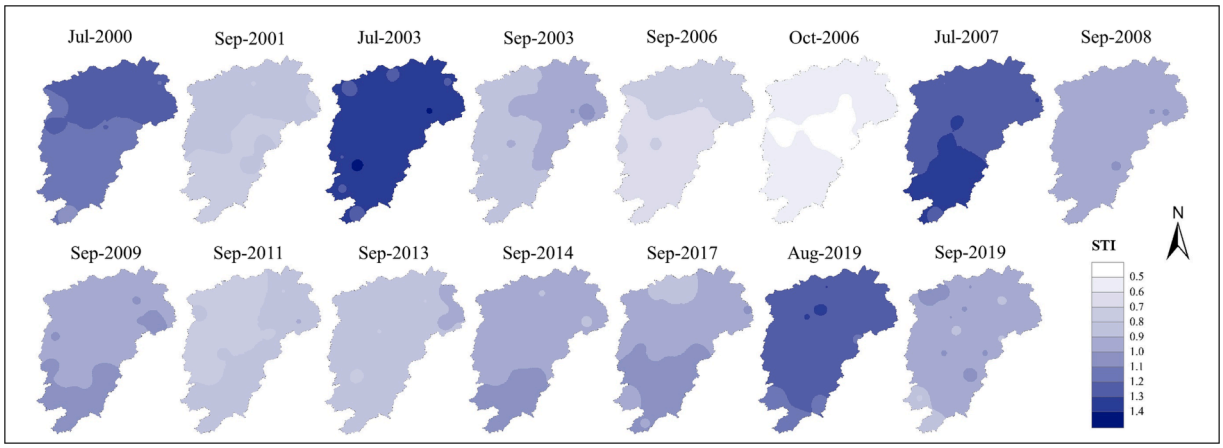

Fig. 5. Spatial patterns of heat events.

explanatory power (q) of the effect of heat events on CV was largest at 0.191 and the lowest was 0.153 for BLF.

The spatial correlations between drought (heat) events and V_{NDVI} showed that most drought events were positively correlated with V_{NDVI} for different vegetation types. Thus, V_{NDVI} was smaller when the drought event was stronger, thereby indicating that drought events mainly inhibited the growth of vegetation. In addition, we found that some drought events were negatively correlated with V_{NDVI}, which contributed to vegetation growth, but the q values for the influence of these drought events on V_{NDVI} were generally small. For example, the q values were all small for the effects of the first, 13th, and 14th drought events on CV, and similar results were also found for other types of vegetation. The consistency of the direction of the effect of heat events on changes in the growth of vegetation was significantly worse than that for drought events, and vegetation exhibited more irregular responses (positive and negative effects were chaotic). In general, V_{NDVI} was negatively correlated with more heat events, thereby indicating that heat events mainly inhibited the growth of vegetation.

3.3. Delayed impacts of drought and heat events on vegetation growth

The delayed responses of five major vegetation types in PYLB to drought and heat events were also investigated. We calculated the average value of the explanatory power (q) for the effects of 15 drought and heat events on different types of vegetation in the current month, as well as with one month lag and two months lag. The lag period corresponding to the maximum value of the average explanatory power is the optimal response time of vegetation to drought (heat) events, and it indicates the lagged impact of extreme events, which reflects the sensitivity of vegetation to different types of drought (heat) stress (Shi et al., 2022).

We found that the lagged effects of drought and heat events on vegetation varied among the vegetation types. As shown in Table 1, the maximum mean explanatory power for the effects of drought events on GL and SL were 0.116 and 0.159, respectively, thereby indicating no significant lagged effect of drought events. By contrast, the responses of CV, NLF, and BLF to drought events had lag times of 1–month, 2–months, and 2–months, respectively. SL exhibited no significant lagged response to heat events, and the other four types of vegetation had lagged response times of 2 months to heat events. NLF, BLF, and SL had the same lag times in response to the effects of drought and heat events, but CV and GL responded faster to drought events than heat events, and GL responded significantly more rapidly.

3.4. The effect of compound drought and heat events on vegetation growth

Fig. 7 shows the single factor explanatory power and interactions for the effects of 15 drought and heat events on vegetation during 1998–2019. As shown in (Fig. 7), the average interaction effect of drought and heat events on vegetation was 0.35, which was obviously greater than those for the individual extreme events (0.170 and 0.160, respectively), thereby indicating an obvious interaction between drought and heat events. The interactions clearly amplified the damaging effects of compound events compared with individual

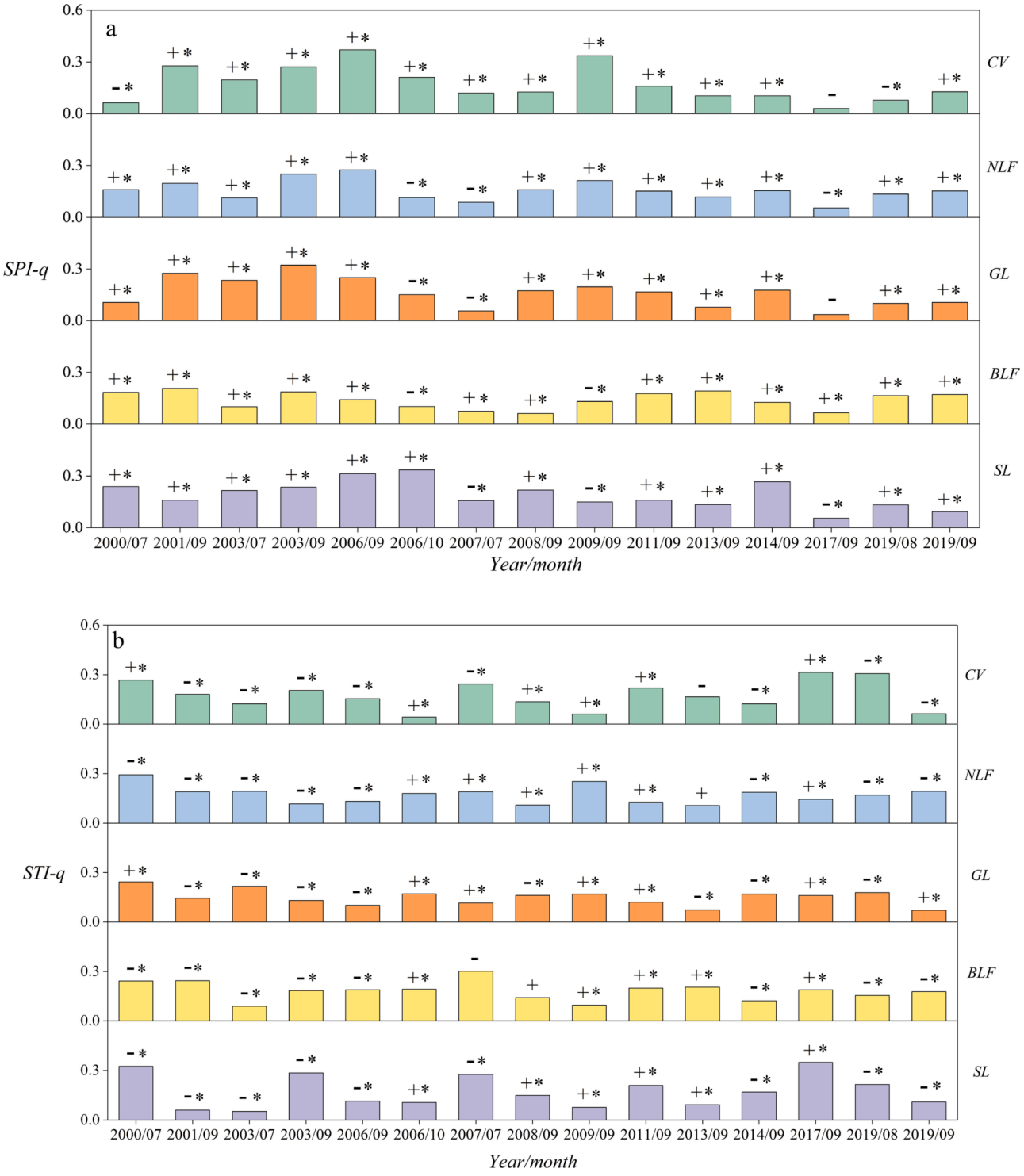

Fig. 6. Effects of drought and heat events on V_{NDVI} during 1998–2019. (a) Effects of drought events and (b) heat events. Note: + indicates that the spatial correlation between drought (heat) events and V_{NDVI} was positive, - indicates that the spatial correlation between drought (heat) events and V_{NDVI} was negative, and * indicates that they passed the 95 % significance test. CV, NLF, GL, BLF, and SL represent cultivated vegetation, needle-leaf forest, grassland, broadleaf forest, and shrubland respectively.

extreme climate events. In particular, CDHEs had the strongest influence on SL, where the mean q(drought ∩ heat) was 0.396, and the least influence on NLF with a mean q(drought ∩ heat) of 0.323. Table 2 shows the modes of interactions between the different drought and hot events. According to the results obtained by the interaction detector, the interaction mode for the effects of drought and heat events on NDVI was bi-factor enhanced or nonlinear enhanced, which suggests that the interaction between drought and heat events had a greater impact on the growth of vegetation than the single or combined effects of the single factors. For example, in 2001, the influence of compound drought and heat events on CV (q(drought ∩ heat) = 0.504) was larger than the separate effects of drought events (q(drought) = 0.278) and heat events (q(heat) = 0.294), and the interaction was bi-factor enhanced. In addition, the influence of CDHE on SL in 2006 (q(drought ∩ heat) = 0.480)

Table 1
Lagged effects of drought and heat events on different types of vegetation.

Vegetation Types	(drought / heat)	No lag	1-month lag	2-month lag
CV	drought	0.108	**0.122**	0.111
	heat	0.114	0.123	**0.128**
NLF	drought	0.105	0.081	**0.122**
	heat	0.099	0.095	**0.129**
GL	drought	**0.116**	0.087	0.104
	heat	0.107	0.102	**0.116**
BLF	drought	0.095	0.074	**0.116**
	heat	0.099	0.098	**0.120**
SL	drought	**0.159**	0.093	0.122
	heat	**0.143**	0.125	0.129

Note: Shading shows the lag time corresponding to the maximum average explanatory power under drought and heat events. CV, NLF, GL, BLF, and SL represent cultivated vegetation, needle-leaf forest, grassland, broadleaf forest, and shrubland respectively.

was larger than the separate effects of drought events (q(drought) = 0.101) or hot events (q(heat) = 0.348), and the interaction was nonlinear enhanced.

4. Discussion

In this study, SPI and STI indexes were used to identify CDHEs in the PYLB, and geographic detectors were used to quantitatively analyze their relative effects and interactive effects on vegetation growth, which have rarely been reported in previous studies. In general, our results showed that heat events had a greater power for explaining the changes in vegetation than drought events, thereby suggesting that the relative effect of heat events on vegetation was greater than that of drought events. Previous studies obtained similar conclusions where they suggested that the effect of the air temperature on vegetation was greater than that of precipitation in the PYLB (Jiang et al., 2022; Wang et al., 2015b), possibly due to the abundant precipitation in humid areas, where rainfall is not the key factor that promotes or limits the growth of vegetation (Zhang and Zhang, 2019). Different types of vegetation respond differently to drought and heat events. We found that drought events and heat events had small impacts on the forest vegetation types (NLF and BLF) with a lag effect of two months, which indicates that forests are more tolerant of extreme weather conditions than other types of vegetation, as also suggested by Huang and Xia (2019), Zhang et al. (2016), and Baumbach et al. (2017). Huang and Xia (2019) found that

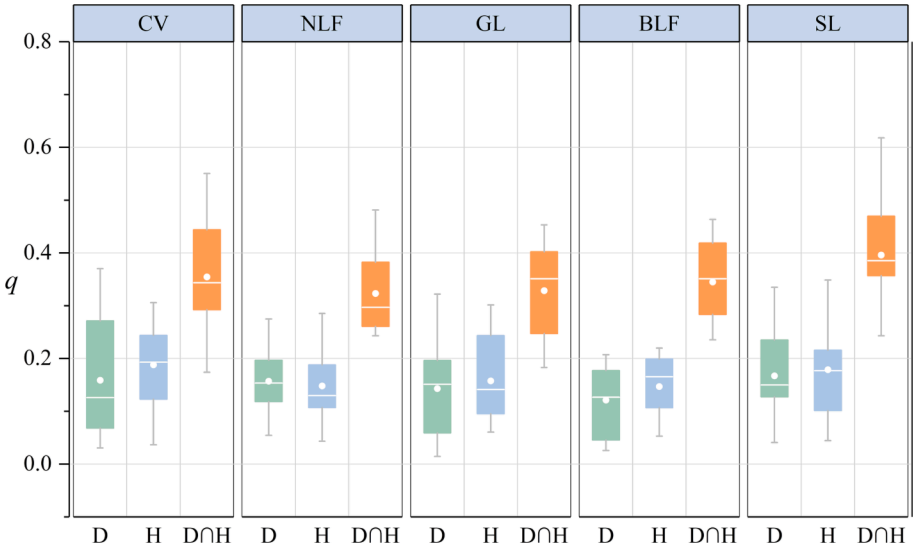

Fig. 7. Box plots showing the single and interactive effects of drought and heat events on vegetation. D represents a drought event, H represents a heat event, and D ∩ H represents a compound drought and heat event. CV, NLF, GL, BLF, and SL represent cultivated vegetation, needle-leaf forest, grassland, broadleaf forest, and shrubland respectively.

Table 2
Interaction modes of effects of different drought events and heat events on vegetation.

Year/month	Interaction modes	CV	NLF	GL	BLF	SL
2000/07	D ∩ H	0.347△	0.375△	0.351△	0.380□	0.471□
2001/09	D ∩ H	0.504□	0.482△	0.434△	0.464△	0.470△
2003/07	D ∩ H	0.444△	0.248△	0.374△	0.363△	0.408△
2003.09	D ∩ H	0.372□	0.348□	0.402□	0.284□	0.386□
2006/09	D ∩ H	0.551□	0.384□	0.372□	0.351△	0.480△
2006/10	D ∩ H	0.333△	0.276△	0.248△	0.293△	0.618□
2007/07	D ∩ H	0.305□	0.243△	0.213△	0.242△	0.428△
2008/09	D ∩ H	0.344△	0.281△	0.417△	0.303△	0.357□
2009/09	D ∩ H	0.479□	0.423△	0.383△	0.444△	0.383△
2011/09	D ∩ H	0.293△	0.342△	0.453△	0.419△	0.389△
2013/09	D ∩ H	0.300△	0.297△	0.255△	0.444△	0.381△
2014/09	D ∩ H	0.243□	0.266□	0.350□	0.263□	0.380□
2017/09	D ∩ H	0.425△	0.383△	0.284△	0.365△	0.257△
2019/08	D ∩ H	0.174△	0.261□	0.183□	0.236□	0.296□
2019/09	D ∩ H	0.209△	0.243□	0.216△	0.329□	0.243△

Note: △ represents nonlinear enhanced (q(drought ∩ heat) > q(drought) + q(heat)) and □ represents bi-factor enhanced (q(drought ∩ heat) > Max(q(drought), q(heat)). CV, NLF, GL, BLF, and SL represent cultivated vegetation, needle-leaf forest, grassland, broadleaf forest, and shrubland respectively.

even under severe drought conditions, BLF was more stable than other types of vegetation (GL and SL). Baumbach et al. (2017) also showed that forests exhibited almost no significant correlations between extreme heat and very low NDVI events, which suggests that they were better able to withstand extreme heat than other types of vegetation. We also found that GL and SL responded more quickly to drought events, probably because they tend to absorb moisture from the topsoil and react rapidly to rainfall changes (Jiang et al., 2022). Similar results were obtained by Zhang et al. (2017) and Shi et al. (2022). Zhang et al. (2017) and Shi et al. (2022) showed that the lag time was shorter in response to drought for GL and SL than woodland. CV comprises shallow-rooted species but the time lag in response to drought was longer compared with GL, probably because irrigation attenuated the sensitivity to drought (Zhan et al., 2022). In particular, we found that most of the drought events had consistent inhibitory effects on the growth of vegetation, and the few drought events that promoted the growth of vegetation usually had smaller values for the explanatory power q. Heat events had highly irregular inhibitory or promoting effects on the growth of vegetation, which may have been related to the different heat preferences of certain vegetation types. Different types of vegetation vary in terms of their water and heat use strategies, rooting habits, xylem structure, and stomatal regulation strategies, which can all affect their tolerance of extreme weather conditions (Xu et al., 2018; Wu et al., 2015). In addition, increases in temperature can affect the growth of vegetation in two ways, where an appropriate amount of warming can boost vegetation growth by increasing the efficiency of photosynthesis (Wang et al., 2015a; Papagiannopoulou et al., 2017), but when the temperature exceeds that tolerated by vegetation the denaturation of enzymes may be accelerated to inhibit growth (Wang and Alimohammadi, 2012; Zhang et al., 2015a; Wang et al., 2021a). Thus, in future studies, additional sample sequences and particular plant species will need to be assessed to further quantify the effects of drought or heat events.

Fig. 7 shows that there was a clear interaction between drought events and heat events, and the impact of CDHEs on vegetation was stronger than that of the individual extreme events. In addition, the characteristic spatial distributions of growing vegetation are generally influenced by the combined effect of drought and heat events. When drought is accompanied by heat, low moisture conditions are generated to exacerbate the negative effects of heat stress, thereby drastically reducing the growth of vegetation (Li et al., 2020; Teskey et al., 2015; Roy et al., 2022). We employed different methods in this study but our findings are consistent with those obtained previously. Compound drought and heat events will have more severe impacts on ecosystems (Zscheischler et al., 2018; Gazol and Camarero, 2022). For example, Feng et al. (2019) showed that when extreme drought (heat) events became CDHEs, the risk of vegetation loss will be increased. Zhu et al. (2021) explored the impacts of high temperature and drought on vegetation growth in China, and showed that the combined impact of high temperature and drought on vegetation productivity was greater than that of drought or high temperature alone. In addition, there are obvious differences between the study areas, which may lead to different conclusions. For example, in arid regions, Kang et al. (2022) studied the influence of CDHEs on the NDVI in Inner Mongolia and found that temperature had the greatest effect on vegetation, followed by CDHEs, and drought had the least significant effect. It is possible that the vegetation has adapted to a prolonged period of low precipitation and is more resistant to drought. In this study, we explored the interaction between drought and heat events, which interacted in a bi-factor enhanced or nonlinear enhanced mode. Interaction patterns are influenced by factors such as drought and heat conditions and vegetation types, so it is necessary to consider different drought and heat conditions and refine the vegetation types in further studies to examine the effects of drought and heat events on vegetation.

We analyzed the PYLB as a typical humid zone to obtain important insights into the response of vegetation to CDHEs in this climatic region. Climate change has increased the probability and extent of drought and heat events, and drought events are often accompanied by heat, and thus the interaction between them amplifies their ecological impacts (Ridder et al., 2022; Wang et al., 2021b). Therefore, it is crucial to consider interactions (compound events) when analyzing the impacts of extreme events. A unique advantage of our method is that the interactions between extreme climate events can be quantified using the geographic detector model, which is not based on linear assumptions and it yields more reliable interaction results than classical regression analysis (Wang and Xu, 2017). Our findings provide new insights into the use of the geographic detector model to explore the effects of compound weather extremes on vegetation and this method can be easily extended to other climatic regions. At present, there are NDVI data sets with longer time series, such as the GIMMS NDVI3g version1 dataset (1982–2015). However, with the increasing degree of climate change, the probability of the appearance of CDHEs increased significantly in the Middle and lower reaches of the Yangtze River of China after 2000 (Gampe et al., 2021; Liu et al., 2022a), and thus the NDVI data set from 1998 to 2019 was collected. It should note that extreme weather events are still frequent after 2019 (Liu et al., 2022b), however, the corresponding meteorological data are inaccessible. Therefore, it is quite necessary to consider recent datasets in future studies to enhance the conclusions. In addition, our study was conducted based on a monthly time scale, where we focused on the short-term effects of CDHEs on vegetation, as well as considering the simultaneous and lagged relationships between drought (heat) events and vegetation, and thus we may have overlooked the cumulative effects of drought and heat events on vegetation. Therefore, the cumulative impacts of extreme climate events need to be investigated in future studies.

5. Conclusions

In this research, we used the geographic detector pattern to quantitatively assess the individual and interactive effects of drought and heat events on vegetation in the PYLB, which is located in a typical humid zone in southern China. The impact of heat events on vegetation was generally stronger than that of drought events in the study area. The responses of different vegetation types to drought (heat) events varied, whereas BLF was more tolerant of drought (heat) events than other vegetation types. Drought events mainly inhibited the growth of vegetation, whereas heat events had mixed effects on inhibiting or promoting the growth of vegetation. SL responded the fastest to drought (heat) events, whereas the responses of NLF and BLF generally had two month lags. The effect of CDHEs on the growth of vegetation (q(drought $\cap$ heat) = 0.35) was significantly stronger than that of the individual extreme events (0.170 and 0.160, respectively), with nonlinear enhanced and bi-factor enhanced interaction modes.

CRediT authorship contribution statement

Huiming Han: Methodology, Formal analysis, Funding acquisition, Writing – original draft. **Hongfu Jian:** Writing – review & editing. **Mingchao Liu:** Data curation, Validation. **Sheng Lei:** Project administration, Resources. **Siyang Yao:** Conceptualization, Methodology, Data curation. **Feng Yan:** Conceptualization, Methodology, Project administration.

Declaration of Competing Interest

The authors declare that they have no known competing financial interests or personal relationships that could have appeared to influence the work reported in this paper.

Data availability

The authors do not have permission to share data.

Acknowledgements

This work was supported by the Science and technology project of Jiangxi Provincial Water Resources Department (202224ZDKT06, 202223YBKT05, 202223YBKT16, 202324YBKT02), Jiangxi Province Science and Technology and Water Conservancy Joint Project (2022KSG01002), and the Jiangxi Key Laboratory of Poyang Lake Water Resources and Environment Open Fund (2022SKSH04).

Appendix A. Supplementary data

Supplementary data to this article can be found online at https://doi.org/10.1016/j.jhydrol.2023.129452.

References

Baumbach, L., Siegmund, J.F., Mittermeier, M., Donner, R.V., 2017. Impacts of temperature extremes on European vegetation during the growing season. Biogeosciences 14 (21), 4891–4903.
Berdugo, M., Delgado-Baquerizo, M., Soliveres, S., et al., 2020. Global ecosystem thresholds driven by aridity. Science 367 (6479), 787–790.
Chen, K., Ge, G., Bao, G., Bai, L., Tong, S., Bao, Y., Chao, L., 2022. Impact of extreme climate on the NDVI of different steppe areas in Inner Mongolia, China. Remote Sens. (Basel) 14 (7), 1530.
Chen, Y., Liao, Z., Shi, Y., Tian, Y., Zhai, P., 2021. Detectable increases in sequential flood-heatwave events across China during 1961–2018. Geophys. Res. Lett. 48 (6).
Diffenbaugh, N.S., Swain, D.L., Touma, D., 2015. Anthropogenic warming has increased drought risk in California. Proc. Natl. Acad. Sci. 112 (13), 3931–3936.
Dong, C., Wang, X., Ran, Y., Nawaz, Z., 2022. Heatwaves significantly slow the vegetation growth rate on the Tibetan Plateau. Remote Sens. (Basel) 14 (10), 2402.
Feng, S., Hao, Z., Zhang, X., Hao, F., 2019. Probabilistic evaluation of the impact of compound dry-hot events on global maize yields. Sci. Total Environ. 689, 1228–1234.
Feng, S., Hao, Z., Wu, X., Zhang, X., Hao, F., 2021. A multi-index evaluation of changes in compound dry and hot events of global maize areas. J. Hydrol. 602.
Fischer, E.M., Sippel, S., Knutti, R., 2021. Increasing probability of record-shattering climate extremes. Nat. Clim. Chang. 11 (8), 689–695.
Gampe, D., Zscheischler, J., Reichstein, M., O'Sullivan, M., Smith, W.K., Sitch, S., Buermann, W., 2021. Increasing impact of warm droughts on northern ecosystem productivity over recent decades. Nat. Clim. Chang. 11 (9), 772–779.
Gazol, A., Camarero, J.J., 2022. Compound climate events increase tree drought mortality across European forests. Sci. Total Environ. 816.
Ge, W., Han, J., Zhang, D., Wang, F., 2021. Divergent impacts of droughts on vegetation phenology and productivity in the Yungui Plateau, southwest China. Ecol. Ind. 127.
Han, D., Wang, G., Liu, T., Xue, B.-L., Kuczera, G., Xu, X., 2018. Hydroclimatic response of evapotranspiration partitioning to prolonged droughts in semiarid grassland. J. Hydrol. 563, 766–777.
Hao, Y., Hao, Z., Feng, S., Zhang, X., Hao, F., 2020. Response of vegetation to El Niño-Southern Oscillation (ENSO) via compound dry and hot events in southern Africa. Global Planet. Change 195.
Huang, K., Xia, J., 2019. High ecosystem stability of evergreen broadleaf forests under severe droughts. Glob. Chang. Biol. 25 (10), 3494–3503.
Jiang, W., Niu, Z., Wang, L., Yao, R., Gui, X., Xiang, F., Ji, Y., 2022. Impacts of drought and climatic factors on vegetation dynamics in the Yellow River Basin and Yangtze River Basin. China. Remote Sensing 14 (4), 930.
Kang, Y., Guo, E., Wang, Y., et al., 2022. Spatiotemporal variation in compound dry and hot events and its effects on NDVI in Inner Mongolia, China. Remote Sens. 14 (16), 3977.
Li, H.W., Li, Y.P., Huang, G.H., Sun, J., 2021. Quantifying effects of compound dry-hot extremes on vegetation in Xinjiang (China) using a vine-copula conditional probability model. Agric. For. Meteorol. 311.
Li, J., Wang, Z., Lai, C., 2020. Severe drought events inducing large decrease of net primary productivity in mainland China during 1982–2015. Sci. Total Environ. 703.
Liu, M., Yin, Y., Wang, X., Ma, X., Chen, Y., Chen, W., 2022a. More frequent, long-lasting, extreme and postponed compound drought and hot events in eastern China. J. Hydrol. 614.
Liu, Z., Zhou, W., Yuan, Y., 2022b. 3D DBSCAN detection and parameter sensitivity of the 2022 Yangtze River summertime heatwave and drought. Atmos. Oceanic Sci. Lett. 100324.
McKee, T., Doesken, N., Kleist, J., 1993. The relationship of drought frequency and duration to time scales. Eighth Conference on Applied Climatology 179–184.
Miller, D.L., Alonzo, M., Meerdink, S.K., Allen, M.A., Tague, C.L., Roberts, D.A., McFadden, J.P., 2022. Seasonal and interannual drought responses of vegetation in a California urbanized area measured using complementary remote sensing indices. ISPRS J. Photogramm. Remote Sens. 183, 178–195.
Nangombe, S., Zhou, T., Zhang, W., et al., 2018. Record-breaking climate extremes in Africa under stabilized 1.5 C and 2 C global warming scenarios. Nature Clim. Change 8 (5), 375–380.
Nemani, R.R., Keeling, C.D., Hashimoto, H., et al., 2003. Climate-driven increases in global terrestrial net primary production from 1982 to 1999. Science 300 (5625), 1560–1563.
Ning, G., Luo, M., Zhang, W., Liu, Z., Wang, S., Gao, T., 2022. Rising risks of compound extreme heat-precipitation events in China. Int. J. Climatol. 42 (11), 5785–5795.
Papagiannopoulou, C., Miralles, D.G., Dorigo, W.A., Verhoest, N.E.C., Depoorter, M., Waegeman, W., 2017. Vegetation anomalies caused by antecedent precipitation in most of the world. Environ. Res. Lett. 12 (7).
Peng, W., Kuang, T., Tao, S., 2019. Quantifying influences of natural factors on vegetation NDVI changes based on geographical detector in Sichuan, western China. J. Clean. Prod. 233, 353–367.
Reichstein, M., Bahn, M., Ciais, P., et al., 2013. Climate extremes and the carbon cycle. Nature 500 (7462), 287–295.
Ridder, N.N., Ukkola, A.M., Pitman, A.J., et al., 2022. Increased occurrence of high impact compound events under climate change. npj Climate Atmos. Sci. 5 (1), 1–8.
Rita, A., Camarero, J.J., Nolè, A., Borghetti, M., Brunetti, M., Pergola, N., Serio, C., Vicente-Serrano, S.M., Tramutoli, V., Ripullone, F., 2020. The impact of drought spells on forests depends on site conditions: the case of 2017 summer heat wave in southern Europe. Glob. Chang. Biol. 26 (2), 851–863.
Rousta, I., Olafsson, H., Moniruzzaman, M.d., Zhang, H., Liou, Y.-A., Mushore, T.D., Gupta, A., 2020. Impacts of drought on vegetation assessed by vegetation indices and meteorological factors in Afghanistan. Remote Sens. (Basel) 12 (15), 2433.
Roy, P., Pal, S.C., Chakrabortty, R., Chowdhuri, I., Saha, A., Shit, M., 2022. Climate change and groundwater overdraft impacts on agricultural drought in India: Vulnerability assessment, food security measures and policy recommendation. Sci. Total Environ. 849.
Shi, X., Ding, H., Wu, M., Zhang, N.a., Shi, M., Chen, F., Li, Y.i., 2022. Effects of different types of drought on vegetation in Huang-Huai-Hai River Basin, China. Ecol. Indic. 144.
Skinner, C.B., Poulsen, C.J., Mankin, J.S., 2018. Amplification of heat extremes by plant CO2 physiological forcing. Nat. Commun. 9 (1), 1–11.
Sungmin, O., Bastos, A., Reichstein, M., et al., 2022. The role of climate and vegetation in regulating drought-heat extremes. J. Clim. 1 (aop), 1–21.
Tan, Z., Tao, H., Jiang, J., Zhang, Q.i., 2015. Influences of climate extremes on NDVI (normalized difference vegetation index) in the Poyang Lake Basin, China. Wetlands 35 (6).
Teskey, R., Wertin, T., Bauweraerts, I., et al., 2015. Responses of tree species to heat waves and extreme heat events. Plant Cell Environ. 38 (9), 1699–1712.
Vicente-Serrano, S.M., Beguería, S., López-Moreno, J.I., 2010. A multiscalar drought index sensitive to global warming: the standardized precipitation evapotranspiration index. J. Clim. 23 (7), 1696–1718.
Wang, D., Alimohammadi, N., 2012. Responses of annual runoff, evaporation, and storage change to climate variability at the watershed scale. Water Resour. Res. 48 (5).
Wang, C., Guo, H., Zhang, L.i., Liu, S., Qiu, Y., Sun, Z., 2015a. Assessing phenological change and climatic control of alpine grasslands in the Tibetan Plateau with MODIS time series. Int. J. Biometeorol. 59 (1), 11–23.
Wang, S., Li, R., Wu, Y., Zhao, S., 2022. Effects of multi-temporal scale drought on vegetation dynamics in Inner Mongolia from 1982 to 2015, China. Ecol. Indic. 136.
Wang, R., Lü, G., Ning, L., Yuan, L., Li, L., 2021b. Likelihood of compound dry and hot extremes increased with stronger dependence during warm seasons. Atmos. Res. 260.
Wang, J., Xu, C., 2017. Geodetector: principle and prospective. Acta Geograph. Sin. 72 (1), 116–134 in Chinese.
Wang, J., Wang, K., Zhang, M., Zhang, C., 2015b. Impacts of climate change and human activities on vegetation cover in hilly southern China. Ecol. Eng. 81, 451–461.
Wang, H., Yan, S., Liang, Z.e., Jiao, K., Li, D., Wei, F., Li, S., 2021a. Strength of association between vegetation greenness and its drivers across China between 1982 and 2015: regional differences and temporal variations. Ecol. Ind. 128.
Wu, X., Jiang, D., 2022. Probabilistic impacts of compound dry and hot events on global gross primary production. Environ. Res. Lett. 17 (3).
Wu, H., Su, X., Singh, V.P., 2021. Blended dry and hot events index for monitoring dry-hot events over global land areas. Geophys. Res. Lett. 48 (24).
Wu, D., Zhao, X., Liang, S., Zhou, T., Huang, K., Tang, B., Zhao, W., 2015. Time-lag effects of global vegetation responses to climate change. Glob. Chang. Biol. 21 (9), 3520–3531.
Xiong, S.i., Guo, F., Zhao, Q., Huang, L., He, L., Zhang, T., 2021. An investigation of extreme weather impact on precipitable water vapor and vegetation growth—a case study in Zhejiang China. Remote Sens. (Basel) 13 (18), 3576.
Xu, C., McDowell, N.G., Fisher, R.A., Wei, L., Sevanto, S., Christoffersen, B.O., Weng, E., Middleton, R.S., 2019. Increasing impacts of extreme droughts on vegetation productivity under climate change. Nat. Clim. Chang. 9 (12), 948–953.
Xu, H.-J., Wang, X.-P., Zhao, C.-Y., Yang, X.-M., 2018. Diverse responses of vegetation growth to meteorological drought across climate zones and land biomes in northern China from 1981 to 2014. Agric. For. Meteorol. 262, 1–13.
Zhan, C., Liang, C., Zhao, L.u., Jiang, S., Niu, K., Zhang, Y., 2022. Drought-related cumulative and time-lag effects on vegetation dynamics across the Yellow River Basin, China. Ecol. Indic. 143.
Zhang, K.e., Kimball, J.S., Nemani, R.R., Running, S.W., Hong, Y., Gourley, J.J., Yu, Z., 2015a. Vegetation greening and climate change promote multidecadal rises of global land evapotranspiration. Sci. Rep. 5 (1).

Zhang, Q., Kong, D., Singh, V.P., Shi, P., 2017. Response of vegetation to different time-scales drought across China: Spatiotemporal patterns, causes and implications. Global Planet. Change 152, 1–11.
Zhang, Y., Voigt, M., Liu, H., 2015b. Contrasting responses of terrestrial ecosystem production to hot temperature extreme regimes between grassland and forest. Biogeosciences 12 (2), 549–556.
Zhang, Y., Piao, S., Sun, Y., Rogers, B.M., Li, X., Lian, X.u., Liu, Z., Chen, A., Peñuelas, J., 2022. Future reversal of warming-enhanced vegetation productivity in the Northern Hemisphere. Nat. Clim. Chang. 12 (6), 581–586.
Zhang, L.i., Xiao, J., Zhou, Y.u., Zheng, Y.i., Li, J., Xiao, H., 2016. Drought events and their effects on vegetation productivity in China. Ecosphere 7 (12), e01591.
Zhang, X., Zhang, B., 2019. The responses of natural vegetation dynamics to drought during the growing season across China. J. Hydrol. 574, 706–714.
Zhao, A., Zhang, A., Liu, J., Feng, L., Zhao, Y., 2019. Assessing the effects of drought and "Grain for Green" Program on vegetation dynamics in China's Loess Plateau from 2000 to 2014. Catena 175, 446–455.
Zhou, Z., Liu, S., Ding, Y., Fu, Q., Wang, Y., Cai, H., Shi, H., 2022. Assessing the responses of vegetation to meteorological drought and its influencing factors with partial wavelet coherence analysis. J. Environ. Manage. 311.
Zhu, X., Zhang, S., Liu, T., Liu, Y., 2021. Impacts of heat and drought on gross primary productivity in China. Remote Sens. (Basel) 13 (3), 378.
Zscheischler, J., Seneviratne, S.I., 2017. Dependence of drivers affects risks associated with compound events. Sci. Adv. 3 (6), e1700263.
Zscheischler, J., Orth, R., Seneviratne, S.I., 2017. Bivariate return periods of temperature and precipitation explain a large fraction of European crop yields. Biogeosciences 14 (13), 3309–3320.
Zscheischler, J., Westra, S., van den Hurk, B.J.J.M., Seneviratne, S.I., Ward, P.J., Pitman, A., AghaKouchak, A., Bresch, D.N., Leonard, M., Wahl, T., Zhang, X., 2018. Future climate risk from compound events. Nat. Clim. Chang. 8 (6), 469–477.